American Mineralogist, Volume 64, pages 1265–1271, 1979

Structure and symmetry of CuS_2 (pyrite structure)

HUBERT E. KING, JR.[1] AND CHARLES T. PREWITT

Department of Earth and Space Sciences
State University of New York
Stony Brook, New York 11794

Abstract

X-ray diffraction data collected on a single-crystal specimen of CuS_2 show that despite its optical anisotropy CuS_2 apparently has the cubic pyrite structure, with $a = 5.7891(6)$A. Precession and Weissenberg photographs fail to reveal any reflections which violate the requirements for space group *Pa*3. Such reflections, however, were observed in four-circle diffractometer measurements, but they are shown to result from multiple diffraction effects. Refinement of the structure in space group *Pa*3 using 209 intensity data gives a weighted residual of 0.014 and $x(S) = 0.39878(5)$. A comparison of the refined structure with other pyrite structures suggests that copper in CuS_2 has a formal valence of 2+ and three antibonding electrons. Also, the CuS_6 octahedron is only slightly distorted, which is in contrast with the square-planar coordination usually found for Cu^{2+}.

Introduction

Disulfides of the transition elements Mn through Zn crystallize in the pyrite structure. The Mn, Fe, Co, and Ni members of this group occur as minerals, and their structures have been refined. CuS_2 and ZnS_2 are not found in nature, but they have been synthesized at high temperatures and pressures. This paper reports the results obtained in a study of the crystal structure and optical properties of CuS_2.

CuS_2 is of interest for two reasons. First, its crystal chemistry is unique. Nakai *et al.* (1978) have shown through X-ray photoelectron spectroscopy that most copper sulfides contain only Cu^+; however, our crystal-chemical evidence indicates that copper in CuS_2 is divalent. The copper is coordinated by six sulfur atoms in a trigonal antiprism slightly distorted from an octahedron, rather than in its usual square-planar coordination. Second, optical evidence for non-cubic symmetry has been reported (Taylor and Kullerud, 1972), but not explained in terms of the crystal structure. Similar, but less intense, optical effects have been reported for FeS_2 (Stanton, 1975; Gibbons, 1967). These authors disagree as to whether the anisotropy is entirely a surface feature or intrinsic to the crystal structure. There is also disagreement with respect to the X-ray diffraction studies on FeS_2. Finklea *et al.* (1976) found no deviations from cubic symmetry, but Bayliss (1977) concluded that at least some pyrite crystals are triclinic. Because optical anisotropy has always been observed for CuS_2 we decided to investigate its crystal structure to provide further information on this intriguing problem.

Experimental

The CuS_2 crystal used is a small ($0.13 \times 0.12 \times 0.08$ mm) rectangular prism selected from material reported by Bither *et al.* (1968). Although polished sections of these crystals are anisotropic in reflected light, long-exposure precession and Weissenberg photographs failed to reveal any diffraction spots which are inconsistent with the requirements for space group *Pa*3. This crystal was mounted on a Picker four-circle diffractometer and its lattice parameters were determined from twelve automatically-centered reflections using Mo$K\alpha$ radiation. The least-squares refinement of the orientation matrix (Tichý, 1970) provides an unconstrained estimate of all unit-cell lengths and angles; with the precision obtained, the geometry of the cell is cubic with $a = 5.7891(6)$A. This value agrees well with previous determinations using X-ray powder diffraction techniques: $a = 5.7898$A (Bither *et al.*, 1968) and $a = 5.7897$A (Taylor and Kullerud, 1972).

[1] Present address: IBM T.J. Watson Research Center, P.O. Box 218, Yorktown Heights, New York, 10598.

0003–004X/79/1112–1265$02.00

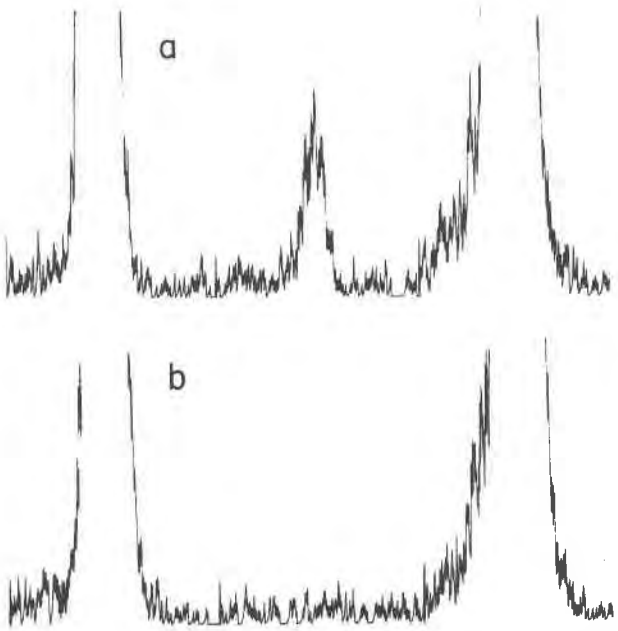

Fig. 1. θ–2θ scans for 400, 500 and 600 at two positions around the diffraction vector: $\Psi = 0°$ (1a) and $\Psi = 151°$ (1b). Ψ is a right-handed rotation whose zero is defined when $\omega = 0$ with an (hkl) plane in diffracting position.

With the crystal mounted on the diffractometer, we again tested for reflections which violated $Pa3$ symmetry. To minimize multiple diffraction effects, we used graphite monochromated Mo$K\alpha$ radiation and an arbitrarily-oriented crystal ([1,0.1,$\overline{0.8}$] was approximately parallel to the Φ axis). The θ–2θ scan mode was used. Even with this arbitrary orientation, we observed, as Bayliss had for FeS_2, several forbidden reflections (an example for 500 is shown in Fig. 1a). However, all the forbidden reflections we observed could be eliminated by rotating the crystal around the diffraction vector to some arbitrary Ψ angle (Fig. 1b). Ψ is a right-handed rotation whose zero is defined with $\omega = 0$ with an (hkl) plane in diffracting position. Further information was provided by making integrated intensity measurements at every 0.5° in Ψ from −90 to +90° and plotting the results as $I_{obs}/2\sigma_I$ *vs.* Ψ (Fig. 2). This figure shows that, even though the diffracted intensity is above the detection limit ($I_{obs}/2\sigma_I = 1$ in this figure) at some Ψ values, it is below that limit at many other Ψ values. Because a Bragg reflection's intensity should not become undetectable at any Ψ value, we conclude that all such observed reflections, forbidden for space group $Pa3$, are the result of multiple diffraction effects. We also believe that, although Bayliss (1977) may have been working with non-cubic FeS_2 crystals, he did not give sufficient information to eliminate the possibility that the extra reflections he observed were caused by multiple diffraction.

Coppens (1968) discussed criteria for the occurrence of multiple Bragg scattering, and concluded that reciprocal lattice points within $0.003A^{-1}$ of the Ewald sphere could satisfy the requirements for multiple diffraction. In order to test the applicability of this idea to FeS_2 and CuS_2, we calculated the number of reciprocal lattice points which meet this criterion for various sets of diffraction conditions. For the 100

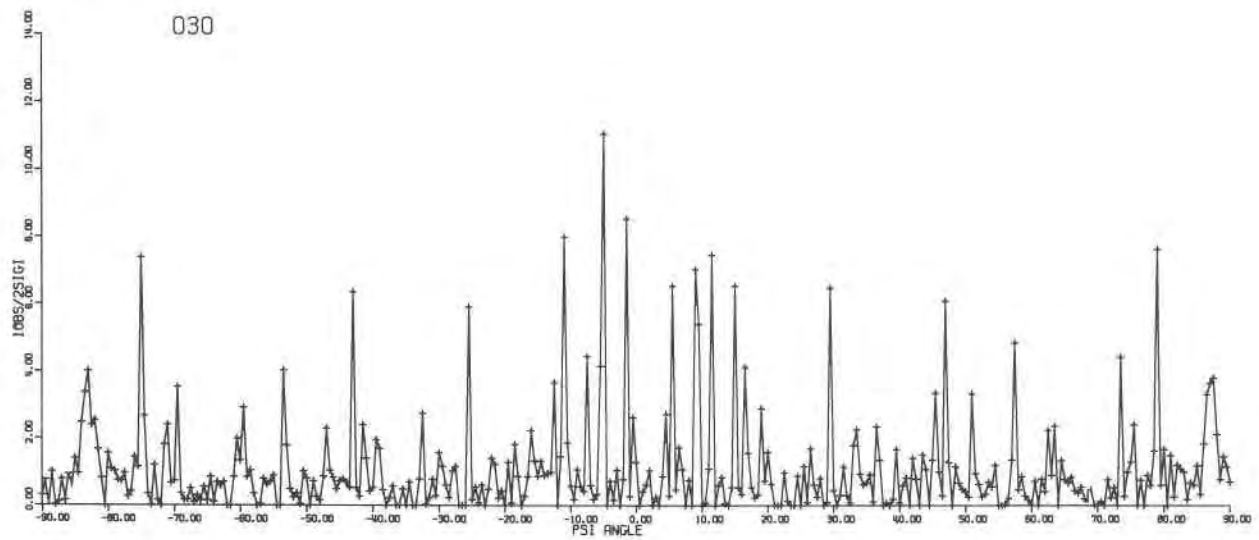

Fig. 2. Results of integrated intensity measurements at every 0.5° around the diffraction vector from −90 to 90°. The intensity is normalized to the detection limit ($2\sigma_I$); thus, a value >1 is considered to be observed.

Table 1. Refinement results

Space group	$P2_1/a\bar{3}$-T_h^6
No. of reflections	251
No. of observed reflections*	209
Wtd. r, all data**	0.014
R, all data+	0.019
Wtd. r, observed reflections	0.014
R, observed reflections	0.013
S++	1.75

*Reflections with $I < 2\sigma_I$ are not included in the observed reflections.

**Wtd. $r = [\Sigma w(|F_o|-|F_c|)^2/\Sigma wF_o^2]^{1/2}$.

+$R = \Sigma||F_o|-|F_c||/\Sigma|F_o|$.

++Standard deviation of an observation of unit weight.

and 300 reflections of CuS_2 (Mo$K\alpha$ radiation), there are many reflections within 0.003A of the Ewald sphere in any orientation tried thus far. When b^* is initially parallel to the X-ray beam and c^* is normal to the equatorial plane, there are 47 other reciprocal lattice points near the sphere when 100 is in diffracting position. Similar results are obtained for FeS_2. Therefore, it would be extremely difficult, using four-circle geometry, to prove that the extra reflections are a result of causes other than multiple diffraction.

Diffraction intensities for structure refinement were measured on a Picker four-circle diffractometer at the Geophysical Laboratory (Washington, D.C.), using Nb-filtered Mo$K\alpha$ radiation with the diffractometer operating in the θ–2θ scan mode. 253 reflections were measured representing all with $h, k, l > 0$ and $0° < 2\theta < 60°$, except for certain $hk0$ which were inadvertently omitted. Scan rates and background counting times were adjusted for each reflection (Finger *et al.*, 1973) to produce a value of 0.01 for σ_I/I. Reference reflections showed no significant variations during the course of the data collection. Intensities were corrected for Lorentz and polarization effects as well as absorption. The absorption correction was computed using a modified version of Burnham's (1966) program with the mass absorption coefficients of Cromer and Liberman (1970). This program also calculates a geometric factor (Zachariasen, 1967) used in the extinction correction.

Refinement

The program RFINE4 (Finger and Prince, 1975) was used for full-matrix least-squares refinement. Neutral scattering factors of Cromer and Mann (1968) along with anomalous dispersion coefficients of Cromer and Liberman (1970) were used. Equivalent reflections were not averaged to allow for refinement of anisotropic extinction. Only reflections with $I > 2\sigma_I$ were used in the refinement.

The structure was refined in space group $Pa3$ using starting parameters from previous unpublished refinements. In the pyrite structure, the metal atom is at the origin and the nonmetal one at x, x, x; thus, there is one variable positional parameter. The starting model was one having isotropic temperature factors and no correction for secondary extinction. Subsequent models included anisotropic thermal motion and both isotropic (Zachariasen, 1967) and anisotropic (Coppens and Hamilton, 1970; Thornley and Nelmes, 1974) secondary extinction corrections. The final model contained corrections for anisotropic thermal motion and anisotropic type 2 extinction. These refinement results are shown in Table 1, and the observed and calculated structure factors are available.[2] Table 2 gives the final positional parameters, anisotropic temperature factor coeffi-

[2] To receive a copy of this material, order Document AM-79-114 from the Business Office, Mineralogical Society of America, 2000 Florida Avenue, N.W., Washington, D.C. 20009. Please remit $1.00 in advance for the microfiche.

Table 2. Final parameters from the refined model: positional parameters, anisotropic temperature-factor coefficients, equivalent isotropic temperature factors (Hamilton, 1965), and rms displacements along the unique directions calculated from the anisotropic temperature factor corrections

Atom	Site	$x = y = z$	$\beta_{11}=\beta_{22}=\beta_{33}$*	$\beta_{12}=\beta_{13}=\beta_{23}$	B(Eq.)	rms displacement (A) ∥[111]	⊥[111]
Cu	4*b*	0	0.00732(8)+	0.00032(5)	0.98(1)	0.116(1)	0.1090(8)
S	8*c*	0.39878(5)	0.00635(9)	-0.00085(7)	0.85(1)	0.089(2)	0.1106(7)

*The temperature factor expression is $\exp\{-\Sigma\Sigma h_i h_j \beta_{ij}\}$.

+One standard deviation in parentheses.

Table 3. Tensor components (W_{ij}) and the resulting principal axis lengths and directions from refinement of type 2 anisotropic secondary extinction

W_{11}*	W_{22}	W_{33}	W_{12}	W_{13}	W_{23}
4.5(5)	4.0(4)	4.6(6)	-1.8(5)	1.4(2)	1.0(7)

Domain radius (A)	Crystallographic direction
2598	[$\bar{5}.0$, 2.6, $\bar{1}.4$]
1376	[$\bar{2}.9$, $\bar{4}.0$, 2.9]
1263	[$\bar{0}.4$, 3.2, 4.8]

* $\times 10^{-9}$ cm^2.

cients, and the equivalent isotropic temperature factors (Hamilton, 1959). Neither the addition of third cumulant temperature factor coefficients for sulfur nor refinement with the disulfide as a rigid group improved the fit.

Secondary extinction

The secondary extinction model used to correct these data is a modification of the Zachariasen (1967) model by Coppens and Hamilton (1970). The anisotropic correction is significant at the 99.9 percent level (Hamilton, 1965) over the isotropic one (wtd. r = 0.017). The extinction correction is given by (Zachariasen's equation 1)

$$P = P_k y \tag{1}$$

where P is the integrated intensity, P_k the kinematical approximation and y the extinction factor. In RFINE 4,

$$y = [1 + \beta(\theta)\, F_c^2 r^*]^{-1/2} \tag{2}$$

where $\beta(\theta)$ is a geometric factor, calculated for each reflection during the absorption correction, and r^* is a refineable parameter. For the type 2 anisotropic extinction model, r^* is replaced with

$$r^* = (\mathbf{N}^T \mathbf{W}\, \mathbf{N})^{-1/2} \tag{3}$$

N is a unit vector and **W** a second-rank tensor whose components are varied during the refinement. According to the model, this tensor represents an ellipsoidal-shaped, ideal-crystal domain. The $\mathbf{W}_{ij}$ components and the resulting ellipsoid's principal axes lengths and orientations for CuS_2 are given in Table 3. Although this extinction model seems to adequately correct for the effects in our data, recent discussions of extinction (Becker, 1977; Lawrence, 1977) make us doubt that a physical interpretation of the ellipsoid in Table 3 is justified.

Because $\beta(\theta)$ is always positive, equations 1 and 2 show that $r^* > 0$, yet Bayliss (1977) obtained $r^* = -0.156 \times 10^{-4}$ from his refinement of FeS_2. The extinction parameter is correlated with the temperature factors by interaction with the scale factor. The sense of this effect reduces the temperature factors as r^* is decreased and could have led to the nonpositive temperature factors of Bayliss.

Thermal ellipsoids

The thermal ellipsoids of both the metal and nonmetal atoms in the pyrite structure are constrained to be uniaxial with their unique axes along the cube diagonal. The rms thermal amplitudes in this direction and in the plane normal to it for copper and sulfur are listed in Table 2. The thermal ellipsoid for copper is only slightly anisotropic. The ratio of the largest to the smallest rms displacement is 1.06. Its largest displacement is along the trigonal compression axis of the octahedron. Sulfur's thermal ellipsoid is more an-

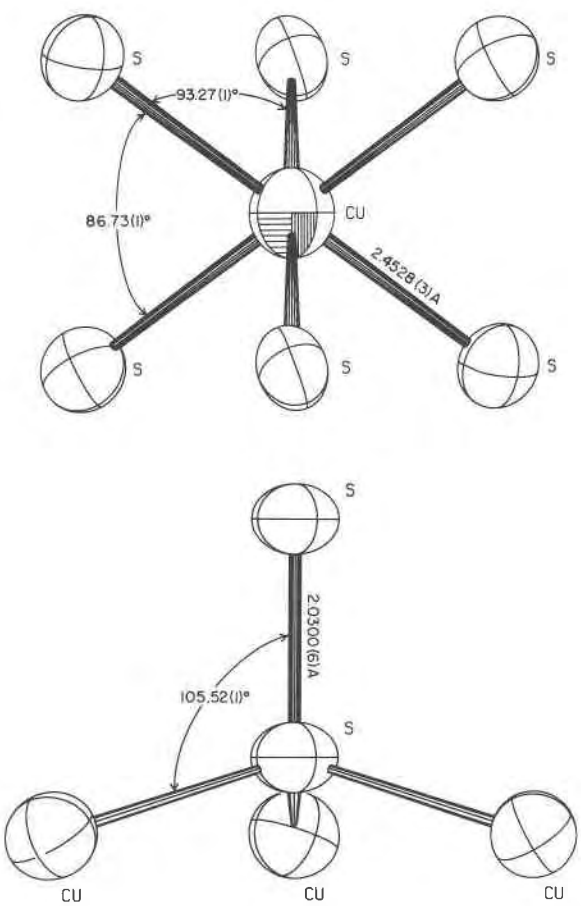

Fig. 3. First coordination poyhedra for Cu and S in CuS_2 with the interatomic distances and angles calculated from the final model.

Table 4. Selected interatomic distances, interatomic angles, and quadratic elongations for several transition element disulfides which have the pyrite structure

	MnS_2 [a]	FeS_2 [b]	CoS_2 [a]	NiS_2 [c]	CuS_2 [d]
M-S, A	2.590	2.259(5)*	2.315	2.401(4)	2.4528(1)
S-S, A	2.086	2.153(6)	2.124	2.059(32)	2.0300(6)
S-S-M, deg	106.1	102.4 (2)	103.3	104.8 (4)	105.52 (2)
S-M-S, deg	86.9	85.66 (9)	86.0	86.5 (1)	86.73 (1)
MS_6 Quadratic Elongation	1.0030	1.0061	1.0052	1.0039	1.0034

[a] *Elliott (1960).*
[b] *Finklea et al. (1976).*
[c] *Furuseth and Kjekshus (1969).*
[d] *This study.*
* *One standard deviation in parentheses.*

isotropic. The ratio of its displacements is 1.24, with the largest displacement normal to the disulfide bond. Apparently, the short sulfur–sulfur distance limits motion along this bond.

Structure

Figure 3 shows the two types of coordination polyhedra in CuS_2. Copper is surrounded by six sulfur atoms in a trigonally-distorted octahedron, and sulfur is coordinated by three copper atoms and one other sulfur atom in a distorted tetrahedron. The CuS_6 octahedra are linked by corner sharing. The sulfur–sulfur distance in pyrite structures approaches that in sulfur itself, and the sulfurs are considered to be bonded to each other.

Some important interatomic distances and angles for the first-row transition-element pyrites are listed in Table 4 and shown in Figure 4. These values show that the parameters for CuS_2 lie along the trends established by the naturally-occurring pyrite structures, and suggest that copper has the same oxidation state (2+) as the other metals in this group. This also suggests that the discussions of bonding in these materials (Bither *et al.*, 1968; Brostigen and Kjekshus, 1970; Goodenough, 1972) are applicable to CuS_2. These models attribute the increase in the metal–sulfur bond length (Fig. 4) to an increase in the number of antibonding electrons. Three are assigned to the copper in CuS_2. In addition, Kjekshus and Nicholson (1971) suggest that these electrons produce a redistribution of electron density which causes the decrease in the sulfur–sulfur bond length (Fig. 4).

Usually, Cu^{2+} is found in square-planar coordination. If the bonding is sufficiently ionic, this can be ascribed to Jahn–Teller distortion. However, Jahn–Teller distortion is unusual in transition-metal sulfides because of extensive electron delocalization (Vaughan and Craig, 1978) and, in fact, the amount of octahedral distortion in pyrite structures (compression along the trigonal axis) appears to be a function of size of the metal atoms. Quadratic elongation values (Robinson *et al.*, 1971) in Table 4 show that FeS_2 has the most distorted octahedron of any member of

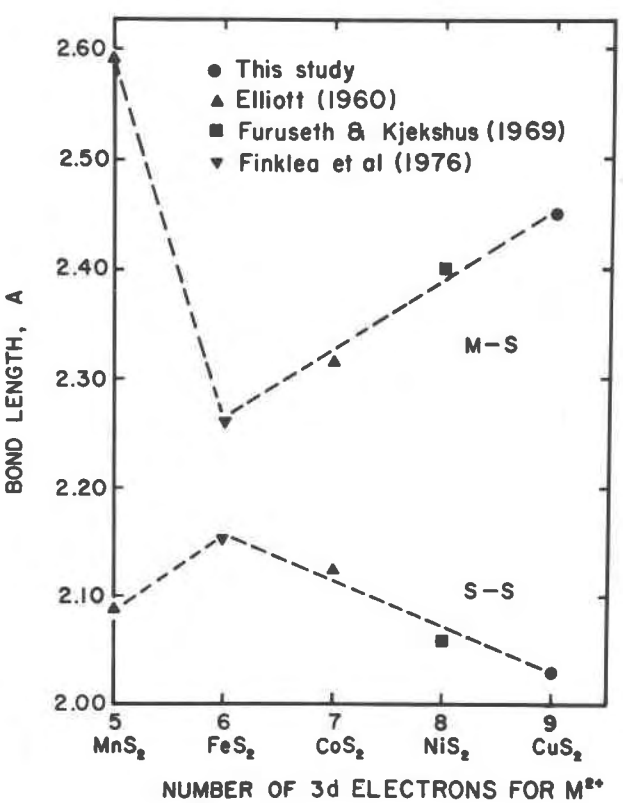

Fig. 4. Bond-length variation for first-row transition-element disulfide pyrite structures including the CuS_2 results.

this series and that the distortion decreases through CuS_2.

Non-cubic symmetry

The optical anisotropy observed for CuS_2 and FeS_2 has raised questions about the correct symmetry for these structures. If this anisotropy were a function of the deviation from cubic symmetry, CuS_2 should not be cubic. The anisotropy is ubiquitous for CuS_2 and usually it is more intense than that for FeS_2. Although the refinement presented here cannot prove that CuS_2 is cubic, it can be used to test other models. The final model has 12 variable parameters, 209 data, and a weighted residual of 0.014. With few variables and a low residual, it is difficult to obtain a statistically significant improvement in the refinement through decreasing the symmetry (increasing the number of variables). For example, one lower-symmetry model suggested by optical data (Gibbons, 1967) is a trigonal structure with its c axis along one of the cube diagonals in the pyrite unit cell. We refined the CuS_2 data in the $R\bar{3}$ space group with the c axis along $[11\bar{1}]$ of pyrite. That model has 23 variable parameters and gives a residual of 0.016. A residual of 0.013 would be necessary for a significant improvement (95 percent confidence level; Hamilton, 1965) over the cubic model.

These arguments suggest that the optical anisotropy is a surface effect. When we examined polished sections of our material, we observed an increase in the intensity of these optical effects with time. After a month's exposure to air, the intensity of the anisotropy was noticeably greater than that of a freshly polished sample. One possibility is that epitaxial growth of a second phase causes the anisotropy. Samples of FeS_2 and CuS_2 were polished, exposed to air for variable lengths of time, and examined with a scanning electron microscope. The results to date are inconclusive. A second phase was observed on some samples, but we have not been able to obtain repeatable results.

Conclusions

Although polished sections of CuS_2 are optically anisotropic, no structural evidence has been found for symmetry lower than cubic. A similar anisotropy in FeS_2 may indicate that some of these crystals are not cubic. However, we believe the refinement by Bayliss does not adequately test this possibility. Trends established by naturally-occuring pyrites suggest that copper in CuS_2 behaves similarly to the metals in other pyrites: it has a 2+ formal valence and three antibonding electrons. The refined structure shows that the CuS_6 octahedron is only slightly distorted, which probably indicates crystal field distortions are not important for these materials.

Acknowledgments

We thank Larry W. Finger for collecting some of the X-ray data used in this study and for discussions concerning secondary extinction effects. We also thank Robin Reichlin who performed the scanning electron microscope experiments. This research was supported by NSF grant EAR 77-13042.

References

Bayliss, P. (1977) Crystal structure refinement of a weakly anisotropic pyrite. *Am. Mineral., 62*, 1168–1172.

Becker, P. (1977) The theoretical models of extinction. Their domain of applicability. *Acta Crystallogr., A33*, 243–249.

Bither, T. A., R. J. Bouchard, W. H. Cloud, P. C. Donohue and W. J. Siemons (1968) Transition metal pyrite dichalcogenides. High-pressure synthesis and correlation of properties. *Inorg. Chem., 7*, 2208–2220.

Bröstigen, G. and A. Kjekshus (1970) Bonding schemes for compounds with pyrite, marcasite and arsenopyrite type structures. *Acta Chem. Scand., 24*, 2993–3012.

Burnham, C. W. (1966) Computation of absorption corrections, and the significance of end effect. *Am. Mineral., 51*, 159–67.

Coppens, P. (1968) The elimination of multiple reflection on the four-circle diffractometer. *Acta Crystallogr.*, A24, 253–257.

——— and W. C. Hamilton (1970) Anisotropic extinction corrections in the Zachariasen approximation. *Acta Crystallogr., A26*, 71–83.

Cromer, D. T. and D. Liberman, (1970) Relativistic calculation of anomalous scattering factors for X-rays. *J. Chem. Phys.*, 53, 1891–1898.

——— and J. B. Mann (1968) X-ray scattering factors computed from numerical Hartree–Fock wave functions. *Acta Crystallogr., A24*, 321–324.

Elliott, N. (1960) Interatomic distances in FeS_2, CoS_2 and NiS_2. *J. Chem. Phys., 33*, 903–905.

Finger, L. W., C. G. Hadidiacos and Y. Ohashi (1973) A computer automated, single-crystal X-ray diffractometer. *Carnegie Inst. Wash. Year Book, 72*, 694–699.

——— and E. Prince (1975) A system of Fortran IV computer programs for crystal structure computations. *Natl. Bur. Stand. Tech. Note 854.*

Finklea, S. L., III, Le Conte Cathey and E. L. Amma (1976) Investigation of the bonding mechanism in pyrite using the Mössbauer effect and X-ray crystallography. *Acta Crystallogr., A32*, 529–537.

Furuseth, S. and A. Kjekshus (1969) On the magnetic properties of $CoSe_2$, NiS_2, and $NiSe_2$. *Acta Chem. Scand., 23*, 2325–2334.

Gibbons, G. S. (1967) Optical anisotropy in pyrite. *Am. Mineral., 52*, 359–370.

Goodenough, J. (1972) Energy bands in TX_2 compounds with pyrite, marcasite, and arsenopyrite structures. *J. Solid State Chem.*, 5, 144–152.

Hamilton, W. C. (1959) On the isotropic temperature factor equivalent to a given anisotropic temperature factor. *Acta Crystallogr., 12*, 609–610.

——— (1965) Significance tests on the crystallographic R-factor. *Acta Crystallogr., 18*, 502–510.

Kjekshus, A. and D. G. Nicholson (1971) The significance of π back-bonding in compounds with pyrite, marcasite, and arsenopyrite type structures. *Acta Chem. Scand., 25*, 866–876.

Lawrence, J. L. (1977) A critique of Zachariasen's theory of extinction. *Acta Crystallogr., A33*, 232–234.

Nakai, I., Y. Sugitani, K. Nagashima and Y. Niwa (1978) X-ray photo-electron spectroscopic study of copper minerals. *J. Inorg. Nucl. Chem., 40*, 789–791.

Robinson, K., G. V. Gibbs and P. H. Ribbe (1971) Quadratic elongations: a quantitative measure of distortion in coordination polyhedra. *Science, 172*, 567–570.

Stanton, R. L. (1975) Studies of polished surfaces of pyrite and some implications. *Can. Mineral., 6*, 87–118.

Taylor, L. A. and G. Kullerud (1972) Phase equilibria associated with the stability of copper disulfide. *Neues Jahrb. Mineral. Monatsh.*, 458–464.

Thornley, F. R. and R. J. Nelmes (1974) Highly anisotropic extinction. *Acta Crystallogr., A30*, 748–757.

Tichý, K. (1970) A least-squares method for the determination of the orientation matrix in single-crystal diffractometry. *Acta Crystallogr., A26*, 295–296.

Vaughan, D. J. and J. R. Craig (1978) *Mineral Chemistry of Metal Sulfides.* Cambridge University Press, New York.

Zachariasen, W. H. (1967) A general theory of X-ray diffraction in crystals. *Acta Crystallogr., 23*, 558–564.

Manuscript received, March 19, 1979;
accepted for publication, July 16, 1979.